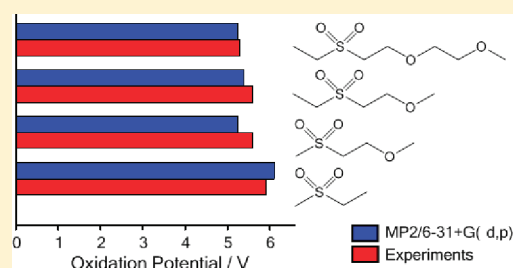


Electrochemical Windows of Sulfone-Based Electrolytes for High-Voltage Li-Ion Batteries

Nan Shao,[†] Xiao-Guang Sun,[†] Sheng Dai,^{†,‡} and De-en Jiang^{*,†}[†]Chemical Sciences Division, Oak Ridge National Laboratory, Oak Ridge, Tennessee 37831, United States[‡]Department of Chemistry, University of Tennessee, Knoxville, Tennessee 37966, United States Supporting Information

ABSTRACT: Further development of high-voltage lithium-ion batteries requires electrolytes with electrochemical windows greater than 5 V. Sulfone-based electrolytes are promising for such a purpose. Here we compute the electrochemical windows for experimentally tested sulfone electrolytes by different levels of theory in combination with various solvation models. The MP2 method combined with the polarizable continuum model is shown to be the most accurate method to predict oxidation potentials of sulfone-based electrolytes with mean deviation less than 0.29 V. Mulliken charge analysis shows that the oxidation happens on the sulfone group for ethylmethyl sulfone and tetramethylene sulfone, and on the ether group for ether functionalized sulfones. Large electrochemical windows of sulfone-based electrolytes are mainly contributed by the sulfone group in the molecules which helps lower the HOMO level. This study can help understand the voltage limits imposed by the sulfone-based electrolytes and aid in designing new electrolytes with greater electrochemical windows.



1. INTRODUCTION

Electrolytes in batteries, capacitors, and fuel cells are a medium to transfer ions between a pair of electrodes.¹ A practical lithium ion battery requires that the electrochemical potential (EP) of the anode is lower than the lowest unoccupied molecular orbital (LUMO) of the electrolyte, and EP of cathode is higher than the highest occupied molecular orbital (HOMO) of the electrolyte, unless a stable passivating solid electrolyte interphase (SEI) forms on the electrode. Therefore, the electronic structures of the salt and the solvent composing the electrolyte limit the selection of cathode and anode materials with high voltage applications. To find electrolyte with large electrochemical windows, especially for the solvent in the electrolyte, becomes one of the challenges for further development of lithium rechargeable batteries.² In addition, the Li-ion conductivity, electronic conductivity, and physical properties such as viscosity, density, and melting point are all important factors for a good electrolyte.

Experimentally, the electrochemical window of an electrolyte for Li-ion batteries is normally defined as the onset of the oxidation potential in cyclic voltammetry scanned from low to high voltage. Conventional solvents of nonaqueous electrolytes are organic carbonates with electrochemical windows <5.0 V,^{3,4} such as the linear carbonates (dimethyl carbonate, diethyl carbonate, etc.) and cyclic carbonates (propylene carbonate, ethylene carbonate, etc.). However, with the development of new high-voltage (≥ 5 V) cathode materials,^{5–7} new electrolytes need to be developed.

In response to the challenges of electrolytes, the unsymmetric acyclic sulfone-based electrolytes have become one of the state-of-the-art electrolytes with high electrochemical stability

(>5.0 V).^{8–13} Dimethyl sulfone, one simplest of the sulfone family, is a highly polar molecule but with a relatively high melting point (108.9 °C). Adding unsymmetric aliphatic groups can lower the melting point. For example, ethylmethyl sulfone (EMS) was reported to have a melting point of 36.5 °C and an electrochemical window of 5.8 V vs Li^+/Li .⁸ More unsymmetric sulfones with different length of oligo(ethyleneglycol) segments have been synthesized^{9–11} with even lower melting points. The excellent electrochemical stabilities of sulfone-based electrolytes have been confirmed by various applications.^{13–15} For example, tetramethylene sulfone (TMS) and EMS were examined in the $\text{LiTi}_5\text{O}_{12}/\text{LiNi}_{0.5}\text{Mn}_{1.5}\text{O}_4$ cell by Abouimrane et al.¹³ EMS was also found to be capable of supporting the complete delithiation process of a layered transition metal oxide cathode up to 5.4 V.¹⁵

Complementary to the experiments, quantum mechanical calculations can provide insights into the electrochemical windows of electrolytes from the perspective of their electronic structures. Computational studies of the one-electron oxidation potentials of benzene derivatives,¹⁶ organic and inorganic fluorine-containing anions,¹⁷ ether solvent molecules,¹⁸ and reduction potentials of nitroaromatic compounds,^{19,20} have been reported. Recently, Maeshima et al. studied the electrochemical potential windows of six molecules for electric double-layer capacitors using the Hartree–Fock method and isodensity polarizable continuum model (IPCM).²¹ Good agreement with the experiment was achieved.

Received: May 11, 2011

Revised: September 14, 2011

Published: September 15, 2011

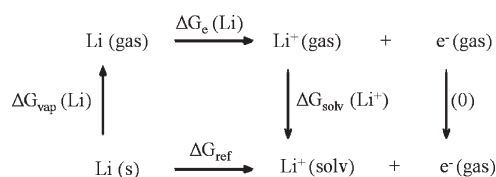


Figure 1. Free energy cycle for computing the oxidation potential of the Li^+/Li reference.

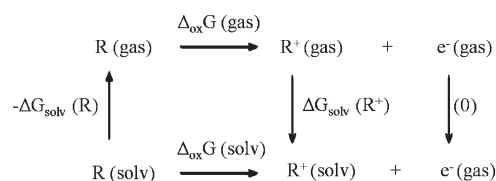


Figure 2. Free energy cycle for computing the oxidation potential of a solvent molecule R .

The progress in the experimental exploration of high-voltage electrolytes for Li-ion batteries and the recent computational studies of redox properties of organic molecules in liquids prompted us to examine the electrochemical windows of sulfone-based electrolytes from a quantum mechanical perspective. The goal is twofold: to benchmark various levels of theory for an accurate way to predict electrochemical windows for sulfone electrolytes and to understand what leads to their high electrochemical windows. Following the computational method used (section 2), we will present results for five sulfone molecules whose oxidation potentials have been measured (section 3). We will summarize and conclude in section 4.

2. COMPUTATIONAL METHODOLOGY

It is generally accepted that the salt used in an electrolyte is much more difficult to oxidize than the neutral solvent molecule, so in our modeling of the electrolyte electrochemical window we focus on the solvent. We assume that the salt in the electrolyte plays a secondary role, and therefore, we did not consider it in this work. To determine the electrochemical window (that is, the oxidation potential in our case) of solvent molecules, thermodynamic cycles for both the lithium reference and the electrolyte oxidation reactions were applied (see Figures 1 and 2).^{16–20,22}

The oxidation process is assumed to be a one-electron transfer from a solvent molecule (R) to the electrode, leaving a radical cation (R^+). For the Li^+/Li reference, the process is as follows.

The free energy for Li^+/Li oxidation process is given by eq 1:

$$\Delta G_{\text{ref}} = \Delta G_{\text{vap}}(\text{Li}) + \Delta G_{\text{e}}(\text{Li}) + \Delta G_{\text{soln}}(\text{Li}^+) \quad (1)$$

In eq 1, the free energy of vaporization of Li , $\Delta G_{\text{vap}}(\text{Li})$, is the tabulated quantity of 118.0 kJ/mol.²³ The free energy of ionization of Li , $\Delta G_{\text{e}}(\text{Li})$, and the free energy of solvation, $\Delta G_{\text{soln}}(\text{Li}^+)$ were calculated by the same level of theory as for the electrolytes. The respective dielectric constants were applied to each $\Delta G_{\text{soln}}(\text{Li}^+)$. For the electrolyte's oxidation process, we use the following thermodynamic cycle.

According to the cycle in Figure 2, free energy of oxidation potential in solution is calculated by eq 2

$$\Delta_{\text{ox}} G(\text{soln}) = \Delta_{\text{ox}} G(\text{gas}) + \Delta G_{\text{soln}}(\text{R}^+) - \Delta G_{\text{soln}}(\text{R}) \quad (2)$$

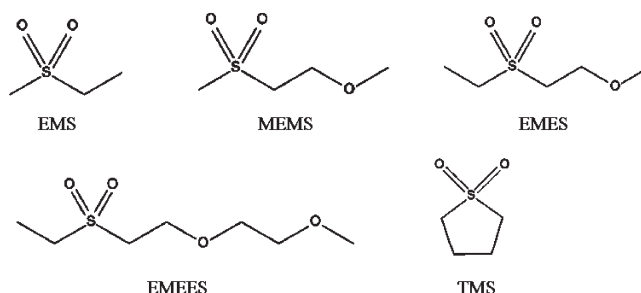


Figure 3. Molecular structures of five sulfones examined in this study: ethylmethyl sulfone (EMS), methoxyethylmethyl sulfone (MEMS), ethylmethoxyethyl sulfone (EMES), ethylmethoxyethoxyethyl sulfone (EMEES), and tetramethylene sulfone (TMS).

The Gibbs free energy change of ionization of the molecules in the gas phase is given by eq 3

$$\Delta_{\text{ox}} G(\text{gas}) = G(\text{R}^+(\text{gas})) + G(\text{e}^-(\text{gas})) - G(\text{R}(\text{gas})) \quad (3)$$

The free energy of the electron, $G(\text{e}^-(\text{gas}))$, is canceled when we reference the electrolyte's oxidation potential against the Li^+/Li reference from eq 1. The standard oxidation potential (a positive number means external voltage put on the electrolyte) relative to the Li^+/Li reference electrode is related to the standard free energy change of the reaction by eq 4

$$E^\circ[\text{V}](\text{versus } \text{Li}^+/\text{Li}) = (\Delta_{\text{ox}} G[\text{eV}] - \Delta G_{\text{ref}}[\text{eV}])/F \quad (4)$$

where F is the Faraday constant ($= 1 \text{ eV/V}$). Oxidation potentials were computed for four recently synthesized sulfone-based electrolytes:^{8,11,12} EMS, MEMS, EMES, and EMEES (Figure 3). Also included is tetramethylene sulfone (sulfolane, or TMS), a cyclic sulfone explored earlier.²⁴

Full geometry optimizations were performed on gas-phase molecules at the HF,²⁵ B3LYP,^{26,27} PBE,²⁸ and MP2^{29,30} levels of theory, with a medium level 6-31+G(d,p) basis set that gives good reproducibility of redox potentials of ion-pairs and the anodic stability of fluorine-containing anions.^{17,21} Harmonic vibrational frequencies were computed and, unless specified, all optimized structures on the potential energy surface are local minima with no imaginary frequencies. The solvation energies were obtained by utilizing self-consistent reaction field (SCRF) methodologies by single-point energy calculation on the gas-phase optimized geometry. Three solvation models were compared: isodensity polarizable continuum model (IPCM),³¹ polarizable continuum model (PCM),³² and the more recent SMD³³ model. The dielectric constants are taken from the reference and experiments.^{9,11,12} The zero-point energy and thermal corrections to the solvation free energy were included.²¹ All calculations were done by the GAUSSIAN09 software package.³⁴

3. RESULTS AND DISCUSSION

3.1. Predicted Oxidation Potentials in Comparison with the Experiments. The experimental electrochemical window in Li-ion battery research usually focuses on the onset of the oxidation process, so the oxidation potential of an electrolyte is measured against the Li^+/Li electrode. Here we briefly review the experimental measurement of oxidation potentials for the five sulfone molecules in Figure 3. They were measured in cyclic voltammetry with Pt as the working electrode and Li foil as reference and counter electrodes; the electrolyte was composed

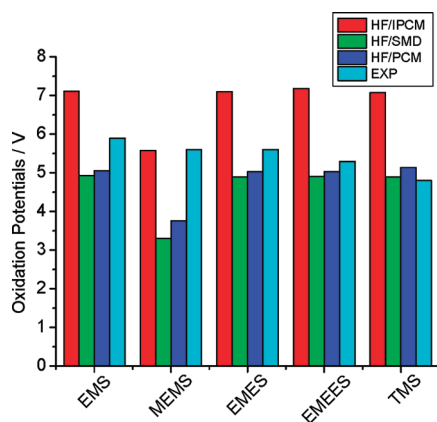


Figure 4. Oxidation potentials calculated at the HF/6-31+G(d,p) level for three solvation models: isodensity polarizable continuum model (IPCM), polarizable continuum model (PCM), and SMD. Experimental oxidation potentials from the literature^{8,11,12} are listed for comparison.

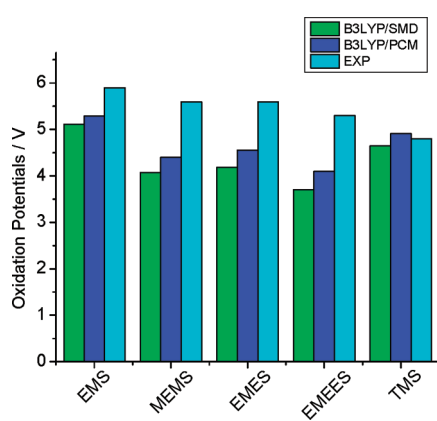


Figure 5. Oxidation potentials calculated at the B3LYP/6-31+G(d,p) level for two solvation models: SMD and PCM. Experimental oxidation potentials from the literature^{8,11,12} are listed for comparison.

of the same salt [Lithium bis(trifluoromethanesulfonyl) imide (LiTFSI)] dissolved in the sulfone solvents (1.0 M); the measured oxidation potentials are 5.89 (EMS),⁸ 5.6 (EMES),¹² 5.6 (MEMS),¹¹ 5.3 (EMEES),¹² and TMS (4.81 V).⁸

We computed the oxidation potentials of those five sulfone molecules (without including the effect of the salt and assuming that the salt anion is more stable than the solvent) at HF, B3LYP, PBE, and MP2 levels of theory for three solvation models (IPCM, PCM and SMD); numerical values for various free energy components and the final oxidation potentials are provided in Tables S1–S4 in the Supporting Information (SI). Figure 4 shows the HF results for the five sulfone molecules. One can see that the predicted oxidation potentials have relative good agreement with the experiments for the PCM and SMD models, except MEMS; the larger error in the case of MEMS might come from the deficiency of electronic correlation effect of the HF method. The PCM model is slightly better than the more recent SMD model, while the IPCM model gives the largest average deviation to the experiment. The poor performance of the IPCM model is due to the large overestimate of the oxidation potential for the Li⁺/Li reference by the IPCM model (see Table S1 in the SI).

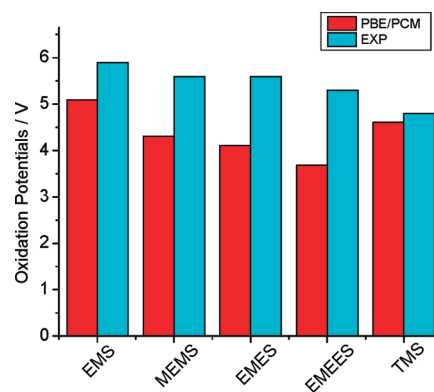


Figure 6. Oxidation potentials calculated at the PBE/6-31+G(d,p) level for the PCM model. Experimental oxidation potentials from the literature^{8,11,12} are listed for comparison.

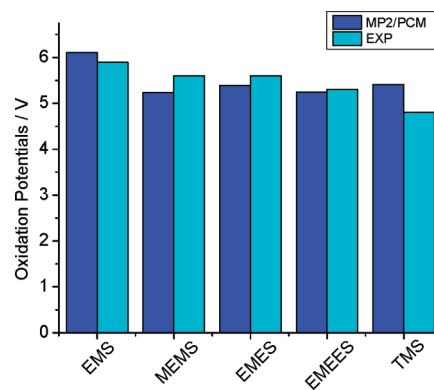


Figure 7. Oxidation potentials calculated at the MP2/6-31+G(d,p)/PCM level for the PCM model (MP2/PCM). Experimental oxidation potentials from the literature^{8,11,12} are listed for comparison.

Figure 5 shows the B3LYP results for the SMD and PCM solvation models. One can see that B3LYP underestimates the oxidation potential more systematically than HF when compared with the experiment, especially for MEMS, EMES, and EMEES which have both sulfone and ether groups. This may be related to the overstabilization of the radical cation by B3LYP. Molecular orbital (MO) analysis shows that the B3LYP HOMOs of MEMS, EMES, and EMEES are all occupied by ether groups. The PCM model again outperforms the SMD model in B3LYP as it does with HF. Since the PCM model is more accurate in both HF and B3LYP results, it was chosen for the following pure DFT and MP2 calculations.

To compare with the hybrid B3LYP, pure DFT with the PBE functional in the PCM model was performed and the results are plotted in Figure 6. One can see that the oxidation potentials from PBE give a larger mean deviation (1.08 V) to the experiments than which from B3LYP (0.8 V), showing that the pure DFT method will overestimate the stability of the cation even more than the hybrid method such as B3LYP. We also examined another pure DFT method, TPSS,³⁵ and similar results to the PBE method were obtained. Both PBE and TPSS energetics are listed in Table S3 in the SI.

The MP2 results in the PCM model are displayed in Figure 7. We found that MP2 full optimization for the gas phase gives the

best agreement with the experiment with a small 0.29 V in mean deviation. The better performance of the MP2 method shows the importance of Hartree–Fock orbitals and electronic correlation to the calculation of oxidation potentials of sulfone-based electrolytes. Since MP2 optimization with the basis set of 6-31+G(d,p) is relatively computationally expensive for large molecules, we tested MP2 single-point energetics based on HF and B3LYP optimized geometries for higher efficiency. Both MP2//B3LYP and MP2//HF methods combined with the PCM model give comparable moderate mean deviations (0.46 and 0.48 V, respectively) to the experiments (see SI Table S4), indicating that they could be applied as preliminary methods in predicting oxidation potentials.

3.2. Molecular Frontier Orbitals of Sulfone Molecules and Change of Atomic Charges after Oxidation. The high oxidation potentials of sulfone molecules that we have reproduced from our quantum mechanical calculations have to do with their HOMO orbital, since during oxidation the electrolyte molecule loses one electron from its HOMO orbital. To

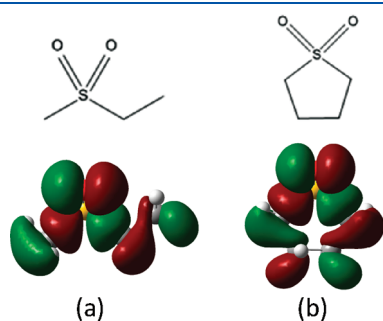


Figure 8. Hartree–Fock HOMO orbitals of (a) EMS and (b) TMS. The isovalue is 0.02 au.

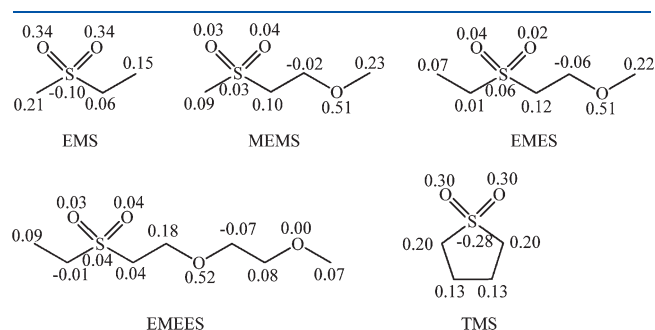


Figure 9. Changes of Mulliken charge on the heavy atoms between the radical cation and the neutral molecule.

understand its characteristics, in Figure 8, we plot the HOMO and HOMO–1 orbitals of EMS and TMS that do not have the ether group. One can see that their HOMO orbital is dominated by the sulfone group; their HOMO–1 orbital is at least 0.7 eV lower in energy. Mulliken charge analysis (see Figure 9) also shows that the oxidation happens mainly on the oxygen in the sulfone group.

For the three ether-containing sulfones, the oxidation happens mainly on the ether oxygen instead of on sulfone (Figure 9). Because the ether is easier to be oxidized than the sulfone group, the ether functionality reduces the oxidation potential. However, the presence of the sulfone group helps mitigate the decrease to the oxidation potential by the ether group due to its strong electron-withdrawing ability. For example, one notes from Figure 9 that in EMEES the ether O group closer to the sulfone group gets oxidized instead of the one far away, indicating a strong effect of the sulfone group on the nearby ether O group. In terms of the degree of the decrease to the oxidation potential by the ether group on the whole molecule, we will discuss it in section 3.4 in terms of the HOMO level.

3.3. Electronic Static Potential. The high oxidation potential of sulfone molecules indicates great difficulty in removing an electron from the molecules containing a highly polar sulfone group. Electronic static potential (ESP) is commonly utilized to display the polarity and stability of molecules. ESP mapped on the isosurface (0.001 au) of electronic density of EMES (as a representative of the ether-functionalized sulfone solvent) was plotted in Figure 10. The very negative electrostatic potential on the sulfone oxygen (–43.5 kcal/mol) and two strong positive electrostatic potential areas along the extension of the oxygen–sulfur covalent bonds (31.2 kcal/mol) lead to a large polarity, which can be explained by the concept of σ -hole.^{36,37} The large polarity of the sulfone group also helps dissolve the Li salt and the high cathodic stability.

3.4. Correlation between the HOMO Energies and the Oxidation Potentials. Since oxidation of an electrolyte happens by losing one electron from the HOMO orbital, it is natural to correlate the oxidation potential to the HOMO level.¹⁷ In Figure 11, we plot the HOMO levels (based on MP2-optimized geometry) against the experimental oxidation potentials. One can see that a roughly linear correlation exists between the HOMO level and the oxidation potential. This is reasonable in that a lower HOMO level indicates a greater difficulty to lose an electron from the orbital. This correlation can be used as a rule of thumb to computationally screen electrolytes for high oxidation potentials. Work is underway to test this hypothesis.

The HOMO level can also be used to understand the lowering of oxidation potential by the ether group to the sulfone molecule.

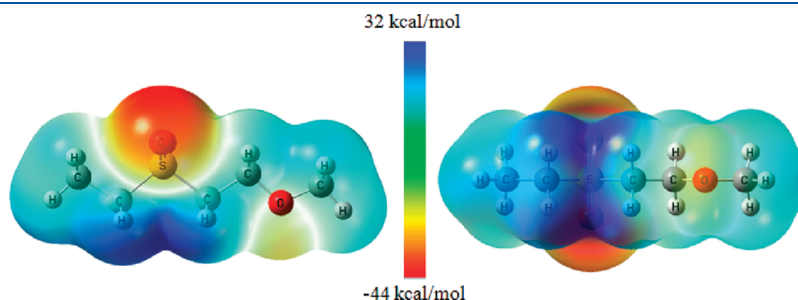


Figure 10. Side view (left) and top view (right) of electrostatic potential for EMES.

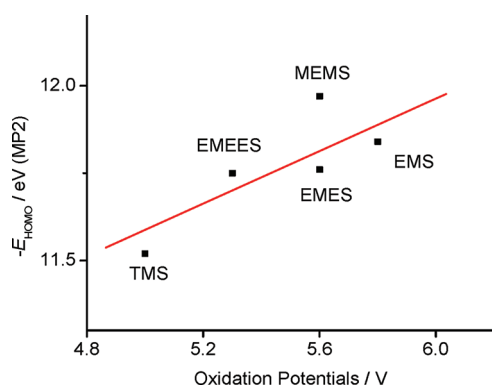


Figure 11. Correlation between the HOMO energies and the experimental oxidation potentials.

For example, EMEES can be viewed as the EMS and DME (dimethoxyethane) molecules linked together with a C–C bond, and the HOMO levels of EMS, EMEES, and DME are -11.84 , -11.76 , and -11.03 V, respectively. Although the ether O group gets oxidized on EMEES (Figure 9), the lowering of its HOMO level by the sulfone group leads to an oxidation potential for EMEES (5.3 V)¹² in between those of EMS (5.9 V)⁸ and DME (4.6 V),³⁸ instead of close to that of DME. This is called a synergistic effect previously,¹² and here we show that the high oxidation potential originates from the lowering of the HOMO level by the sulfone group in comparison with that of the ether. Nevertheless, the ether functionalization does make the oxidation potential worse, even though it helps lower the melting point of sulfone. We are currently pursuing further strategy of functionalization to maintain or increase sulfone's oxidation potential while decreasing its melting point.

4. CONCLUSIONS

We have computed the oxidation potentials of sulfone-based electrolytes at the HF, B3LYP, PBE, and MP2 levels of theory with the 6-31+G(d,p) basis sets. Three solvation models (IPCM, PCM, and SMD) were compared. It was found that the MP2 full optimization with the PCM model can well reproduce the measured oxidation potentials for five sulfone electrolytes examined. Orbital analysis revealed the dominant contribution of the sulfone group to the HOMO orbitals for the nonfunctionalized sulfone molecules. Change of Mulliken charges upon oxidation showed that the ether group gets oxidized for ether-functionalized sulfone molecules, leading to a decreased oxidation potential. But this decrease is somewhat mitigated by the close-by sulfone group. The correlation found between the HOMO level and the oxidation potential provides a useful guide to computationally screen electrolytes for high oxidation potentials.

■ ASSOCIATED CONTENT

S Supporting Information. Numerical values of free energy components in computing the oxidation potentials. This material is available free of charge via the Internet at <http://pubs.acs.org>.

■ AUTHOR INFORMATION

Corresponding Author

*E-mail: jiangd@ornl.gov.

■ ACKNOWLEDGMENT

This work was supported by the Division of Materials Science and Engineering, Office of Basic Energy Sciences, U.S. Department of Energy. This research used resources of the National Energy Research Scientific Computing Center, which is supported by the Office of Science of the U.S. Department of Energy under Contract No. DE-AC02-05CH11231.

■ REFERENCES

- (1) Xu, K. *Chem. Rev.* **2004**, *104*, 4303–4417.
- (2) Goodenough, J. B.; Kim, Y. *Chem. Mater.* **2010**, *22*, 587–603.
- (3) Egashira, M.; Okada, S.; Yamaki, J. *Electrochemistry* **2001**, *69*, 455–457.
- (4) Cattaneo, E.; Ruch, J. J. *Power Sources* **1993**, *44*, 341–347.
- (5) Du, G. D.; Nuli, Y. N.; Yang, J.; Wang, J. L. *Mater. Res. Bull.* **2008**, *43*, 3607–3613.
- (6) Wang, F.; Yang, J.; NuLi, Y. N.; Wang, J. L. *Power Sources* **2010**, *195*, 6884–6887.
- (7) Amine, K.; Yasuda, H.; Yamachi, M. *Electrochem. Solid St.* **2000**, *3*, 178–179.
- (8) Xu, K.; Angell, C. A. *J. Electrochem. Soc.* **1998**, *145*, L70–L72.
- (9) Xu, K.; Angell, C. A. *J. Electrochem. Soc.* **2002**, *149*, A920–A926.
- (10) Sun, X. G.; Angell, C. A. *Solid State Ionics* **2004**, *175*, 257–260.
- (11) Sun, X. G.; Angell, C. A. *Electrochem. Commun.* **2009**, *11*, 1418–1421.
- (12) Sun, X. G.; Angell, C. A. *Electrochem. Commun.* **2005**, *7*, 261–266.
- (13) Abouimrane, A.; Belharouak, I.; Amine, K. *Electrochem. Commun.* **2009**, *11*, 1073–1076.
- (14) Seel, J. A.; Dahn, J. R. *J. Electrochem. Soc.* **2000**, *147*, 892–898.
- (15) Lu, Z. H.; Dahn, J. R. *J. Electrochem. Soc.* **2001**, *148*, A710–A715.
- (16) Han, Y. K.; Jung, J.; Cho, J. J.; Kim, H. J. *Chem. Phys. Lett.* **2003**, *368*, 601–608.
- (17) Ue, M.; Murakami, A.; Nakamura, S. *J. Electrochem. Soc.* **2002**, *149*, A1572–A1577.
- (18) Zhang, X. R.; Pugh, J. K.; Ross, P. N. *J. Electrochem. Soc.* **2001**, *148*, E183–E188.
- (19) Zubatyuk, R. I.; Gorb, L.; Shishkin, O. V.; Qasim, M.; Leszczynski, J. *J. Comput. Chem.* **2010**, *31*, 144–150.
- (20) Phillips, K. L.; Sandler, S. I.; Chiu, P. C. *J. Comput. Chem.* **2011**, *32*, 226–239.
- (21) Maeshima, H.; Moriwake, H.; Kuwabara, A.; Fisher, C. A. *J. Electrochem. Soc.* **2010**, *157*, A696–A701.
- (22) Fu, Y.; Liu, L.; Yu, H. Z.; Wang, Y. M.; Guo, Q. X. *J. Am. Chem. Soc.* **2005**, *127*, 7227–7234.
- (23) Database of National Institute of Standards (<http://webbook.nist.gov/chemistry/>).
- (24) Matsuda, Y.; Morita, M.; Yamada, K.; Hirai, K. *J. Electrochem. Soc.* **1985**, *132*, 2538–2543.
- (25) Pople, J. A.; Nesbet, R. K. *J. Chem. Phys.* **1954**, *22*, 571–574.
- (26) Becke, A. D. *J. Chem. Phys.* **1993**, *98*, 5648–5652.
- (27) Lee, C. T.; Yang, W. T.; Parr, R. G. *Phys. Rev. B* **1988**, *37*, 785–789.
- (28) Perdew, J. P.; Burke, K.; Ernzerhof, M. *Phys. Rev. Lett.* **1996**, *77*, 3865–3868.
- (29) Head-Gordon, M.; Pople, J. A.; Frisch, M. J. *Chem. Phys. Lett.* **1988**, *153*, 503–506.
- (30) Fiolhais, C.; Perdew, J. P. *Phys. Rev. B* **1992**, *45*, 6207–6215.
- (31) Foresman, J. B.; Keith, T. A.; Wiberg, K. B.; Snoonian, J.; Frisch, M. J. *J. Phys. Chem.* **1996**, *100*, 16098–16104.
- (32) Scalmani, G.; Frisch, M. J. *J. Chem. Phys.* **2010**, *132*, 114110.
- (33) Marenich, A. V.; Cramer, C. J.; Truhlar, D. G. *J. Phys. Chem. B* **2009**, *113*, 6378–6396.
- (34) Frisch, M. J.; Trucks, G. W.; Schlegel, H. B.; Scuseria, G. E.; Robb, M. A.; Cheeseman, J. R.; Scalmani, G.; Barone, V.; Mennucci, B.; Petersson, G. A., et al. *Gaussian 09*, revision A; Gaussian, Inc.: Wallingford, CT, 2009.

- (35) Tao, J. M.; Perdew, J. P.; Staroverov, V. N.; Scuseria, G. E. *Phys. Rev. Lett.* **2003**, *91*, 146401.
- (36) Clark, T.; Murray, J. S.; Lane, P.; Politzer, P. *J. Mol. Model.* **2008**, *14*, 689–697.
- (37) Murray, J. S.; Lane, P.; Politzer, P. *J. Mol. Model.* **2009**, *15*, 723–729.
- (38) Ossola, F.; Pistoia, G.; Seeber, R.; Ugo, P. *Electrochim. Acta* **1988**, *33*, 47–50.